https://doi.org/10.5194/egusphere-2024-104
Preprint. Discussion started: 17 January 2024

Changing optical properties of Black Carbon and Brown Carbon aerosols during long-range transport from the Indo-Gangetic Plain to the equatorial Indian Ocean

Krishnakant Budhavant[1,4], Mohanan Remain Manoj[2], Samuel Mwaniki Gaita[2], Henry Holmstrand[2], Abdus Salam[3], Ahmed Muslim[1], Sreedharan Krishnakumari Satheesh[4], Örjan Gustafsson[2]

[1]Maldives Meteorological Services, 02020, Maldives
[2]Department of Environmental Science and the Bolin Centre for Climate Research, Stockholm University, Stockholm 1069, Sweden
[3]Department of Chemistry, University of Dhaka, Dhaka 1000, Bangladesh
[4]Divecha Centre for Climate Change, Indian Institute of Science, Bangalore 560012, India

Correspondence to: Örjan Gustafsson (Orjan.Gustafsson@aces.su.se)

Abstract. Atmospheric aerosols strongly influence the global climate by their light absorption (e.g., black carbon, BC, brown carbon, BrC) and scattering (e.g., sulfate) properties. This study presents simultaneous measurements of ambient aerosol light absorption properties and chemical composition from three large-footprint South Asian receptor sites during the South Asian Pollution Experiment (SAPOEX) in December-March 2018. The BC mass absorption cross-section (BC-MAC_{678}) values increased from 3.5 ± 1.3 at the Bhola Climate Observatory-Bangladesh (i.e., located at exit outflow of Indo-Gangetic Plain) to 6.4 ± 1.3 at the two regional receptor observatories at Maldives Climate Observatory-Hanimaadhoo (MCOH) and Maldives Climate Observatory-Gan (MCOG). This likely reflects a coating-enhancement effect due to ageing of the aerosols during long-range transport. At the same time, the BrC-MAC_{365} decreased by a factor of three from the IGP exit to the equatorial Indian Ocean, likely due to photochemical bleaching of organic chromophores. The high chlorine-to-sodium ratio at the near-source-region BCOB suggests a significant contribution of chorine from anthropogenic activities. This particulate Cl^- has the potential to convert into Cl-radicals that can affect the oxidation capacity of the polluted air. Moreover, Cl^- is shown to be near-fully consumed during the long-range transport. The results of this synoptic study over the large South Asian scale have significance for understanding the ageing effect of the optical and chemical properties of aerosols as the pollution from the Indo-Gangetic Plain disperses over regional scales.

https://doi.org/10.5194/egusphere-2024-104
Preprint. Discussion started: 17 January 2024

1 Introduction

Light-absorbing carbonaceous moieties represent a key component of atmospheric aerosols as they affect global climate due to both their direct absorption and combined/indirect effects with other components (Ramanathan and Carmichael, 2008; IPCC, 2021). The systematic underestimation of the total optical absorption of aerosols by a factor of 2 to 3 in climate models compared to observations-based estimates illustrates the current significant uncertainties and potential systematic bias (Gustafsson and Ramanathan, 2016; Ansari et al., 2023). In addition to climate effects, anthropogenic aerosols such as black carbon (BC) and sulfate (SO_4^{2-}) can penetrate deeply into human lungs and increase the risk of cardiovascular and respiratory diseases (Mauderly et al., 2008; Lelieveld et al., 2015; WHO, 2016).

The aerosol loadings in the South Asian region are much higher than the global average, primarily due to anthropogenic activities. The high anthropogenic aerosol levels exert a strong influence on both the climate and the quality of the air people breathe in South Asia, primarily due to massive emissions from the Indo-Gangetic Plain (IGP), the densely populated and industrialized northern part of India and Bangladesh (Shindell et al., 2012; Nair et al., 2023). Other significant environmental effects of anthropogenic carbonaceous aerosols (BC and OC) over South Asia include "regional dimming" (Ramanathan et al., 2007; Nair et al., 2023), decreased evaporation and rainfall, weakened monsoons (Bollasina et al., 2011), intensification of tropical cyclones (Ramanathan et al., 2007), and melting of the Himalayan glaciers (Ramanathan et al., 2007); its watershed today serves over 3 billion people.

The BC and water-soluble organic carbon (WSOC, with its light-absorbing sub-component brown carbon, BrC) aerosols are mainly emitted from incomplete fossil fuel combustion and biomass burning (Chakrabarty et al., 2008; Höpner et al., 2016; Dasari et al., 2019). The present understanding suggests that BC is less reactive and thus has less change over distance, on the other hand, BrC seems to be bleaching (Dasari et al., 2019). Investigations of the dynamically shifting optical properties of BrC during long-range transport are important for assessing its climate effects. Accurate mass absorption cross-section (MAC) and source apportionment of BC aerosols are also crucial as they are input to climate and air quality models. BC aerosols from fossil versus biomass combustion have different light absorption/radiative effects and atmospheric fates. The emissions, source apportionment and optical properties of anthropogenic aerosols from India and the greater South Asia is a key uncertainty in climate and environment research that urgently needs to be addressed.

Access to the three strategically-located Atmospheric Observatories in South Asia provides an opportunity for synoptic observations of aerosols along the main wintertime flow trajectory from the key source region for anthropogenic aerosols to its dispersal over regional scales of the northern Indian Ocean (Figure 1). The arrows in Figure 1 illustrate the common pathway of the well-pronounced South Asian winter monsoon outflow projected from meteorological back trajectory analyses. During the dry winter season with the highest anthropogenic aerosol loadings (e.g., BC, OC, nss-SO_4^{2-}, nss-K^+), the Himalayas cause topographical steering to force Northern Indian air pollution into the North Bay of Bengal (Figure 1). The main flow is then southward, with many air parcels arriving at Maldives Climate Observatory-Hanimaadhoo (MCOH) and Maldives Climate Observatory-Gan (MCOG).

https://doi.org/10.5194/egusphere-2024-104
Preprint. Discussion started: 17 January 2024

The South Asian Pollution Experiment 2018 (SAPOEX-18) was a large international multi-site and multi-approach campaign with one of the key focal points on the absorption properties of BC and BrC during long-range transport in the South Asian source-receptor system. The current study reports on the ambient evolution of light-absorption properties for both BC and BrC in connection with the chemical composition of aerosols by combining in situ filter measurements, online optical instrument data of aerosol physical and chemical properties, and satellite and remote sensing data sets. Observations were collected over three strategically located regional receptor sites. The Bhola Climate Observatory-Bangladesh (BCOB) is intercepting the integrated outflow of IGP in rural southern Bangladesh by the shores of the Bay of Bengal. The MCOH in a northern atoll of the Maldives and MCOG situated close to the equator in the southernmost Maldivian atoll are ideal locations for intercepting the larger footprint of the South Asian outflow. Synoptic studies between BCOB and the Indian Ocean receptor sites may shed light on the changing aerosol composition and optical/radiative effects during long-range over-ocean transport. Finally, the observational constraints on the aerosol composition and optical properties are used in modelling the radiative effects over the three distinct regimes.

2 Methods

2.1 Aerosol sample collection

The work presented here was conducted at three sites: BCOB (Lat 22.17ºN Lon 90.71ºE), MCOH (6.78ºN, 73.18ºE), and MCOG (0.69 ºS, 73.15ºE) from early December 2017 to end of March 2021. The BCOB is located on Bhola Island (also called Dakhin Shahbazpur) in the delta of the Bay of Bengal, about 300 km south of Dhaka, Bangladesh (Ahmed et al., 2018; Shohel et al., 2018; Dasari et al., 2019). The MCOH is located in the northern part of Hanimaadhoo island (Thiladhummathi Atoll), around 3.1 km^2, with around 1800 inhabitants (Corrigan et al., 2006; Höpner et al., 2016; Budhavant et al., 2023). Measurements are taken from a tower platform at 15 m above sea level, from which air samples are directed to a ground-level, air-conditioned laboratory (Corrigan et al., 2006; Budhavant et al., 2018, 2023). The MCOG is located on the southernmost island of the Maldives, at the equator, 500 km south of the capital city Male' and 800 km from MCOH (Corrigan et al., 2006; Ramanathan et al., 2007). A detailed description of each observatory is available in earlier publications (Corrigan et al., 2006; Stone et al., 2007; Dasari et al., 2019). Aerosol samples were collected on pre-combusted (at 450 ºC) 150 mm diameter quartz filters (Millipore) using high-volume samplers (DIGITEL Elektronik AG, Model DH77 at 500 liter/minute). Blank filters were shipped, stored, and processed identically as samples. Each of these three observatories are instrumented to record spectral Aerosol Optical Depth (AOD) data under the AErosol RObotic NETwork (AERONET) (Holben et al., 1998; Ramanathan et al., 2005; Nair et al., 2023).

2.2 Chemical analysis of aerosol filter samples

The aerosols were analyzed for several carbonaceous components and major ions using standard protocols and suitable techniques (Dasari et al., 2019; Budhavant et al., 2023). The mass concentration of EC (here referred to as BC), OC, and total carbon (TC = BC + OC) were measured with a thermal-optical transmission analyzer (Sunset Laboratory,

https://doi.org/10.5194/egusphere-2024-104
Preprint. Discussion started: 17 January 2024

OCEC analyzer) using the National Institute for Occupational Safety and Health (NIOSH-5040 method) (Birch et al., 1996; Budhavant et al., 2015, 2023). NIST-traceable (Reference Material 8785) laboratory standards verify the accuracy of OC, EC, and TC measurements. No detectable signal was observed for the BC in field blanks. The OC concentration values were blank corrected by subtracting an average field blank (5% of sample signals).

Another portion of each aerosol filter was extracted with 18 M-ohm Milli-Q for analysis of water-soluble inorganic ions by using Ion chromatography (IC, Dionex Aquion, Thermo Scientific). The system contains a guard column and an anion-cation separator column with a primary exchange resign and suppressor column (AERS500/CERS 500). The quality of the data was tested with internal and external reference samples. The analytical error was lower than 4% for the anions and 5% for the cations. A more detailed description can be found in Budhavant et al. (2023).

2.3 Aerosol Absorption Measurements

The relationship between atmospheric concentration and direct radiative forcing by BC is its mass absorption cross-section (MAC). The laser beam (678 nm) of the Sunset Laboratory aerosol carbon analyzer was used to measure the light attenuation (ATN = -ln(I/I_0)) of the aerosols on the filter (Ram and Sarin, 2009). The MAC_{BC} of BC is calculated as (Weingartner et al., 2003; Budhavant et al., 2020)

$$\mathrm{MAC_{BC}} = \frac{ATN}{\mathrm{BC_{loading}} \cdot \mathrm{MS} \cdot \mathrm{R(ATN)}} \quad (1)$$

MS is an empirical multiple scattering correction factor implemented in most filter loading correction schemes. To account for the multiple scattering effects, a factor of 4.5 was selected for estimation (Budhavant et al., 2020). Correction for non-linearity when measuring light absorption through a filter is denoted by R.

$$R = \left(\frac{1}{1.114} - 1\right)\left(\frac{\ln(ATN) - \ln(0.1)}{\ln(0.5) - \ln(0.1)}\right) + 1 \quad (2)$$

The Hitachi U2010 UV-VIS spectrophotometer was used to measure the light absorption of the water-extracted aerosol. The MAC for water-soluble brown carbon (WS-BrC) was then calculated.

$$\mathrm{MAC_{WS-BrC}} = \frac{\mathrm{b_{abs,365}}}{[\mathrm{WSOC}]} \quad (3)$$

where WSOC is the water-soluble organic carbon concentration, $b_{abs,365}$ is the absorption coefficient at 365nm. The absorption Ångström exponent (AAE) was estimated as the slope in a linear regression of the logarithm of the b_{abs} versus the logarithm of the wavelength (λ)

$$\ln|\mathrm{b_{abs}}(\lambda)| = -\mathrm{AAE} \cdot \ln|\lambda| + \mathrm{intercept} \quad (4)$$

The AAE was fitted between 330-400 nm to avoid interference from other light-absorbing solutes, such as ammonium nitrate, sodium nitrate, and nitrate ions (Cheng et al., 2011; Bosch et al., 2014).

https://doi.org/10.5194/egusphere-2024-104
Preprint. Discussion started: 17 January 2024

2.4 Aerosol Radiative Forcing

The radiative forcing of aerosol particles is a major uncertainty factor in understanding the Earth's climate (Ramanathan et al., 2007; IPCC et al., 2021; Lu et al., 2023). The radiative implications of aerosols are quantified in terms of their Direct Aerosol Radiative Effects (DARE). Spectral Aerosol Optical Depth (AOD) data from three stations under the AErosol RObotic NETwork (AERONET) (Hess et al., 1998; Bedareva et al., 2014), ozone (OMI, Ozone Monitoring Instrument), water vapor and surface reflectance (MODIS, Moderate Resolution Imaging Spectroradiometer) and surface reflectance were used in this study. The aerosol optical model (Optical Properties of Aerosols and Clouds, OPAC 3.1), which works based on Mie scattering theory (Hess et al., 1998), was used to estimate the optical properties of newly defined aerosol mixtures (Hess et al., 1998). The AOD from the sun photometers, single scattering albedo (SSA), and asymmetry parameters modeled using the Mie scattering model were used as input to Santa Barbara DISORT Atmospheric Radiative Transfer (SBDART) (Ricchiazzi et al., 1998; Lu et al., 2023). The model uses the complex discrete ordinate method to numerically integrate the radiative transfer equations (Stamnes et al., 1988). A detailed description of this model and approach is available elsewhere (Ramanathan et al., 2005; Satheesh et al., 2002; Nair et al., 2023).

2.5 Air mass back-trajectories and remote sensing

Ten-day air mass back trajectories (AMBTs) were generated at an arrival height of 50m at all three sampling sites (Supplementary (S) figures S1–S4), the NOAA Hybrid Single-Particle Lagrangian Trajectory model (version 4) (Draxler et al., 1997; Draxler, 1999). This study's calculations were based on meteorological data from the Global Data Assimilation System (GDAS). The GDAS is run four times daily (at 0000, 0600, 1200, and 1800 UTC). These individual trajectories were clustered into different geographical regions (Figure 1). The MODIS (Moderate Resolution Imaging Spectroradiometer) satellite-derived FIRMS (Fire Information for Resource Management System) based fire-count data combined with cluster analysis to understand the impact of biomass burning emissions from potential source regions during the sampling period (Figure 1).

3 Results and Discussion

3.1 Atmospheric Transport

The AMBTs, AOD, and active fire data were used as parameters to study the atmospheric transport and geographical source regions in the area. Based on atmospheric transport, we defined two temporal source domains: The influence of the heavily polluted Indo Gangetic Plain (IGP) region (18 December 2017 to 8 February 2018) and the total period of the study. Measurements at BCOB represent an accumulation of IGP sources through air mass transport across N. Pakistan, N. India, and Bangladesh, a region containing many large- and mega-cities, regions of heavy industrialization and rural areas with extensive agricultural burning (Figure 1 and Figure S2). The MCOH and MCOG are situated in the northern Indian Ocean and thus intercept long-range pollutant emissions from South Asia, including the IGP, the western part of India, and the Indian Ocean (Figure S3 and Figure S4). Cluster analysis of AMBTs combined with AOD, satellite measurements, and aerosol chemical composition demonstrated that the wintertime northern Indian

https://doi.org/10.5194/egusphere-2024-104
Preprint. Discussion started: 17 January 2024

Ocean is greatly influenced by anthropogenic aerosols transported from source regions like IGP and the western margin of India.

3.2 Organic and Black Carbon

In general, varying primary and secondary sources combined with short atmospheric residence times of aerosol particles containing a high fraction of organic carbon, result in large regional differences in chemical composition, morphology, mixing state, size, and optical properties. OC was the main component of the carbonaceous aerosol in S Asian winter, accounting for 85 ± 5% of total carbon (TC) at BCOB, 66 ± 9% at MCOH, and 67 ± 9% at MCOG. The OC contribution to TC was highest when the wind came from IGP (Figure 2) and minimum when the wind travelled through oceanic regions at all three sites. The BC and OC are very well correlated (R > 0.74) at all three sampling sites, indicating similar source emissions. However, the average ratio of OC to BC was 6.5 ± 2.1 at BCOB, decreasing markedly to 2.2 ± 1.1 at MCOH, and 2.4 ± 1.8 at MCOG. This large decrease from the exit of the IGP source region (BCOB) to the Indian Ocean receptor sites (MCOH and MCOG) demonstrates that OC/BC ratios were strongly affected by selective processing and/or washout of OC during long-range transport (LRT). The atmospheric lifetime of OC is typically shorter than that of BC (Budhavant et al., 2020). Since OC also represents a more complex mixture, it is subject to more atmospheric transformation than BC, reflected in a larger shift in stable isotope fingerprints of the OC component from source to receptor sites in this region (Dasari et al., 2019; Bosch et al., 2014; Kirillova et al., 2016). The highest concentrations of BC, OC, and nss-SO_4^{2-} aerosols were associated with air masses from IGP and the western margin of India.

We found WSOC was a large yet decreasing portion of the total OC (35 ± 6% at BCOB, 21 ± 10% at MCOH, 16 ± 10% at MCOG) (Figure 3). One previous study reported the fossil fuel contribution to WSOC as 8–22% at MCOH (Bosch et al., 2014). Carbonaceous aerosols derived from fossil fuel combustion may be relatively less water-soluble (WSOC ≥20%) due to less oxygenated organic moieties (Ruellan et al., 2001). The mass fraction of WSOC to OC was observed as an indicator of aerosol photochemical processing in the atmosphere (Dasari et al., 2019). This suggests decreasing OC/BC between IGP exit and after transportation over the ocean, indicating selective washout and bleaching reactions of organic carbon.

3.3 Characteristics of the ionic aerosol components

The chemical composition of the aerosols changed both between sites and over time (Table 1, Figure 2). Filter samples were characterized in terms of major anions (Cl^-, NO_3^-, and SO_4^{2-}) and major cations (Na^+, K^+, Mg^{2+}, Ca^{2+}, and NH_4^+) for the four-month sampling period (Figure 4). The highest concentrations of ions were noted for BCOB, which is expected as the site is situated at the outflow of highly polluted IGP. One exception was SO_4^{2-}. The high concentration of SO_4^{2-} and NH_4^+ at MCOH is mainly from the central and east parts of India and IGP, as these are hotspots of SO_2 since these regions house a cluster of thermal power plants, construction industries, and petroleum refineries as a primary source of SO_2 (Guttikunda et al., 2014; Kuttippurath et al., 2022). The IGP is a hotspot of high anthropogenic aerosol loading due to intense agriculture crop residue burning, biomass burning, open waste burning, industries, and high urban activities (Dasari et al., 2020; Ansari and Ramachandran, 2023).

https://doi.org/10.5194/egusphere-2024-104
Preprint. Discussion started: 17 January 2024

To identify the effect of marine influences on aerosol composition, sea salt corrections were calculated using Na^+ as the reference element (Keene et al., 1986). The nss-SO_4^{2-} fraction to total sulfate was at BCOB (99 ± 1 %, mean ± standard deviation), MCOH (98 ± 1%), and MCOG (86 ± 13%), indicating significant contributions of SO_4^{2-} and SO_2 from diesel combustion and coal-fired power plants in India and Bangladesh. Some of the nss-SO_4^{2-} at MCOH may be due to ocean traffic over the northern Indian Ocean, as the majority of shipping emissions result from the combustion of its fuel that releases SO_x (Sulphur Oxides) and NO_x directly into the atmosphere (Corbett and Koehler, 2003; Gopikrishnan and Kuttippurath, 2021).

In the near-source-region BCOB, there is a very high Cl^-/Na^+ ratio (Figure 4, 4.7 ± 3.5) compared to the other two receptor sites. This suggests that there is a significant amount of Cl^- coming from anthropogenic activities. It is possible that the Cl^- comes from the burning of Cl-containing plastics like polyvinyl chloride (PVC) in open waste burning (Pathak et al., 2023). This particulate Cl^- can be converted into Cl-radicals that can impact the oxidation capacity of the polluted air. Additionally, Cl^- is consumed or removed during LRT due to a reactive form of Cl.

We observed a high correlation ($r \geq 0.7$) between EC, OC, and nss-K^+ in aerosol samples collected at BCOB (Table S1) and MCOH (Table S2). The nss-K fraction to total potassium was observed at BCOB (97 ± 3 %), MCOH (78 ± 13%), and MCOG (42 ± 33%), indicating significant contributions from biomass burning at BCOB and MCOH, as nss-K^+ is considered as a proxy for identifying the regional impact of biomass burning emissions (Andreae, 1983; Paris et al., 2010). High concentrations of nss-SO_4^{2-}, nss-K^+, and NH_4^+ in measured ions and carbon aerosols indicate strong anthropogenic sources in the ambient aerosols over the northern Indian Ocean.

3.4 Black carbon mass absorption cross-section

The impact of BC aerosols on air quality, boundary layer dynamics, and climate depends not only on BC concentration but also on the light absorption characteristics of BC. Moreover, MAC values are crucial to estimate radiative forcing accurately. The MAC of BC is here denoted as "BC-MAC_{678}" During the SAPOEX-18 campaign, the calculated BC-MAC_{678} was found to have a lower average value at BCOB (4.4 ± 1.9 m^2g^{-1}) and higher at the most distant Indian Ocean receptor station MCOG (7.0 ± 1.9 m^2g^{-1}), with MCOH, at shorter over-ocean transport distance having a value of 6.1 ± 1.3 m^2g^{-1} (Figure 3). Hence, the effective BC-MAC_{678} for South Asian aerosols increased with transport/ageing time as it dispersed over the nearby ocean. Lower BC-MAC_{678} values constrained here for the IGP outlet at BCOB may represent less-coated BC in contrast to the more aged particles at MCOG and MCOH, which could have a thicker coating (Figure S6). Such coating-enhancement of the effective BC-MAC_{678} has been suggested earlier (Gustafsson and Ramanathan, 2016; Budhavant et al., 2020, 2023) but not until now clearly constrained using synoptic S. Asian source-receptor observations. We here constrain the BC-MAC_{678} coating-enhancement factor between BCOB and time in the northern Indian Ocean to be 60% (±25%). Note that the total enhancement of BC-MAC_{678} may be even larger as there is very likely already a coating affecting the BC-MAC_{678} at BCOB.

These observational constraints in the S Asian global hotspot region are consistent with global simulation models that suggest that in ~1-5 days, the EC can internally mix with other aerosols (Jacobson et al., 2000). After mixing, the

https://doi.org/10.5194/egusphere-2024-104
Preprint. Discussion started: 17 January 2024

photochemical properties of pure BC will no longer be retained due to the coating of the other aerosols in the atmosphere, such as sulfate, nitrate, and organics.

The changes in MAC_{BC} primarily reflect the formation of coating aerosols. We observed that the coating material changed substantially during the ageing process (Figure 3 and S6), possibly through condensation, coagulation, and heterogeneity. BC aerosols that have travelled for a long distance before reaching the sampling location will have ample opportunity to make coating of secondary aerosol material such as sulfate, nitrate, ammonium, water, and organic material (Gustafsson and Ramanathan, 2016; Cui et al., 2016; Chen et al., 2017). The coating induces an enhancement of absorption by the BC core, sometimes called a lensing effect (Andreae and Gelencser, 2006; Peng et al., 2016). Yuan et al. (2021) demonstrated that the MAC_{BC} values at 870 nm at a rural site (Germany) increased as the coating thickness of BC increased. An increase in absorption by coating can be explained in terms of "absorption amplification". Absorption amplification multiplies the MAC of BC particles (Knox et al., 2009; Zhang et al., 2018). BC-MAC_{678} is approximately 60% higher at both MCOH and MCOG receptor observatories after being transported over the ocean than at BCOB. This enhancement during long-range transport, deduced by the synoptic study system, may be underestimated in model estimates of black carbon's climate effects, and it could contribute to the existing bias between models and observations.

3.5 Light Absorption Properties of Brown Carbon

In addition to BC, BrC also affects the radiative forcing at ultraviolet wavelengths, although its MAC is an order of magnitude less than BC in the visible wavelength range (Bosch et al., 2014; Kirillova et al., 2013). During the campaign, measurements of WS extracts of BrC show significant differences in light absorption characteristics between the three sampling sites. The average MAC measured at 365 nm (BrC MAC_{365}) at BCOB (1.0 ± 0.3 m^2 g^{-1}) was two to three times higher than that measured at MCOH (0.3 ± 0.3 m^2 g^{-1}) and MCOG (0.6 ± 0.3 m^2 g^{-1}) (Figure 4). BrC MAC_{365} measured during this study is broadly in the same range as earlier studies focusing on fewer locations from the same region (Bikkina et al., 2014; Dasari et al., 2019). Primary BrC emitted from biomass burning appears to be more light absorptive than secondary aerosols, MAC values at 405 nm ranged from 0.2 to 1.5 m^2 g^{-1} for humic and fulvic acids and 0.001 to 0.09 for secondary organic aerosols (Lambe et al., 2013), while Chen and Bond (2010) reported a range for primary aerosols from 0.1 to 1.1 m^2 g^{-1} (Chen et al., 2010). The average BrC MAC_{365} measured during this study was lower than values reported from close to sources in megacities such as the 1.8 m^2 g^{-1} for Beijing winter (Cheng et al., 2011), 1.6 ± 0.5 m^2 g^{-1} for Delhi (Kirillova et al., 2014). This indicates that the MAC-BrC decreased by a factor of three from the IGP exit to the equatorial Indian Ocean (Figure 3).

The AAE characterizes the spectral characteristic of BrC. Furthermore, AAE is often used to characterize BrC from coal combustion, biomass, and biofuel burning (Chen and Bond, 2010; Rastogi et al., 2021). The AAE value of BrC is typically reported to be ~1 (fossil fuel emissions), ~7 (biomass burning), and 7-15 for laboratory-generated smoke and smoldering of different types of woods (Hoffer et al., 2006; Chen et al., 2010). The average values of AAE of WS-BrC intercepted at the S Asian receptor observatories were 5.5 ± 2.7 at BCOB, 6.5 ± 2.4 at MCOH, and 4.1 ± 0.5 at MCOG. These compare to AAE values measured at Nepal Climate Observatory-Pyramid (4.9 ± 0.7, Kirillova et al.,

https://doi.org/10.5194/egusphere-2024-104
Preprint. Discussion started: 17 January 2024

2016), in New Delhi in winter (5.1 ± 2.0, Kirillova et al., 2014). However, the AAE values in this study were lower than those previously measured at MCOH in winter (7.2 ± 0.7, Bosch et al., 2014) and in the IGP outflow measured over the Bay of Bengal (9.1 ± 2.5, Bikkina and Sarin, 2013). The results of this synoptic study at a large scale in South Asia are significant for understanding the aging effect of optical and chemical properties of aerosols.

3.6 Aerosol Radiative Forcing

From December to March, the tropical Indian Ocean/atmosphere system provides a natural opportunity to study aerosol radiative forcing influenced by anthropogenic aerosols (Satheesh and Ramanathan, 2000; Nair et al., 2023). This is due to the fact that the Indian Ocean atmosphere receives polluted air that travels from the Indian subcontinent and surrounding regions (Figure 1) (Gustafsson et al., 2009; Budhavant et al., 2018).

The DARF (cloud-free atmosphere) has been estimated over BCOB, MCOH, and MCOG on a monthly basis using aerosol optical properties obtained from the OPAC model in SBDART (Figure 5). The DARF at the top of the atmosphere (TOA, 3 km) and at the surface is calculated by estimating the difference of downward and upward fluxes simulated by the model in the atmosphere conditions with and without aerosols for the three sites. The surface forcings and TOA were both negative at all three sampling stations, indicating cooling effects. Meanwhile, the atmospheric column represented a warming effect. The negative sign depicts the dominant presence of scattering aerosols. The monthly average atmospheric forcing was almost double at BCOB (10.5 ± 3.2 Wm^{-2}) than at MCOG (4.8 ± 2.1 Wm^{-2}) due to more (net absorbing) carbon aerosols loading in the air, implying strong warming in the atmosphere over IGP outflow. High atmospheric forcing in March at BCOB is again associated with high aerosol loading. At MCOH, atmospheric forcing (11.2 Wm^{-2}) was slightly higher in January than BCOB (10.4 Wm^{-2}), as MCOH is influenced significantly by the outflow from continental South Asia (Figure 2 and Figure 3). The atmospheric forcing was almost double at BCOB than MCOG due to more anthropogenic aerosol loading (e.g., BC, NO_3^-, nss-K^+), implying strong warming in the atmosphere over IGP outflow.

4 Summary

The South Asian Pollution Experiment 2018 (SAPOEX-18) utilized access to three strategically located atmospheric receptor observatories to provide synoptic observations of the optical properties of ambient carbonaceous aerosols along the main wintertime flow trajectory from key source regions. These observational constraints revealed opposite trends during long-range transport in BC-MAC (increasing, presumably due to coating enhancement) and BrC-MAC (decreasing, presumably due to photochemical bleaching). The study also found significant anthropogenic chloride emissions from human activities, which can affect the oxidation capacity of polluted air. Models estimating the climate effects of particularly BC aerosols may have underestimated the ambient BC-MAC over distant and extensive receptor areas, which could contribute to the discrepancy between aerosol absorption predicted by models constrained by observations. These findings can be utilized to refine model estimates of radiative forcing from both BC and BrC for the large-emission region of South Asia. This is particularly relevant as the severe air pollution from the Indo-Gangetic Plain spreads over large regional scales over the Indian Ocean.

https://doi.org/10.5194/egusphere-2024-104
Preprint. Discussion started: 17 January 2024

Competing interests

The authors declare that they have no conflict of interest.

Author Contributions

K.B. and Ö.G. conceived the study. K.B. collected the Samples at MCOH, A.S. was responsible for sample collection at BCOB, and A.M. was responsible for sample collection at MCOG. K.B. performed the chemical analysis, with the support of S.M.G. and E.K. M.R. performed the radiative forcing estimations and satellite data analysis. K.B. and Ö.G. interpreted the data and drafted the manuscript. All co-authors provided input on interpretations and early versions of the manuscript.

5. Acknowledgment

Elena Kirillova and Sanjeev Dasari (Stockholm University) are acknowledged for their support during the field campaign. We thank the technical staff at BCOB, MCOH, and MCOG for their continued field support. A special thanks to the Maldives Meteorological Services, and the Government of the Republic of Maldives for the ongoing support of the joint MCOH-MCOG operation. K.B. thanks to the additional support from the Regional Resources Center for Asia and the Pacific (RRC.AP), Asian Institute of Technology (AIT), Thailand. We acknowledge financial support from the Swedish Research Council for Sustainable Development (FORMAS Contract Nr. 2020-01917) and the Swedish Research Council (VR Contract Nos 2017-01601, and 2020-05384).

https://doi.org/10.5194/egusphere-2024-104
Preprint. Discussion started: 17 January 2024

Table 1. Aerosol optical depth (AOD), mass absorption cross-section (MAC) of black carbon (BC) and brown carbon (Br-C), the concentration of BC, organic carbon (OC), water-soluble organic carbon (WSOC), absorption Angstrom exponent (AAE), and concentrations of major ions were measured at the Bhola Climate Observatory-Bangladesh (BCOB), Maldives Climate Observatory- Hanimaadhoo (MCOH), Maldives Climate Observatory-Gan (MCOG) during November 2017 to March 2018.

Site	AOD	BC-MAC_{678} (m^2 g^{-1})	BrC-MAC_{365} (m^2 g^{-1})	BC (μg m^{-3})	OC (μg m^{-3})	WSOC (μg m^{-3})	AAE_{BrC} (330-400nm)	NO_3^- (μg m^{-3})	NH_4^+ (μg m^{-3})	nss-SO_4^{2-} (μg m^{-3})	nss-K^+ (μg m^{-3})
BCOB	0.8 ± 0.3	4.4 ± 1.9	1.0 ± 0.3	3.0 ± 1.3	20 ± 11	6.9 ± 4.0	5.5 ± 2.7	7.6 ± 7.3	3.8 ± 3.2	11 ± 5	2.4 ±1.2
MCOH	0.5 ± 0.2	6.1 ± 1.3	0.3 ± 0.3	1.0 ± 0.5	2.3 ± 1.5	0.5 ± 0.4	6.5 ± 2.4	0.1 ± 0.0	4.2 ± 2.7	11 ± 7	0.4 ± 0.3
MCOG	0.2 ± 0.1	7.0 ± 1.9	0.6 ± 0.3	0.3 ± 0.3	0.7 ± 0.5	0.1 ± 0.1	4.1 ± 0.5	0.3 ± 0.4	0.5 ± 0.8	3.0 ± 2	0.1 ± 0.1
Only during synoptic period (18 December 2017 to 8 February 2018)											
BCOB	0.9 ± 0.4	3.5 ± 1.3	1.0 ± 0.2	3.6 ± 1.0	27 ± 8.7	9.1 ± 2.8	6.4 ± 2.0	12 ± 7.7	2.5 ± 3.5	12 ± 5	2.9 ± 1.0
MCOH	0.5 ± 0.2	6.4 ± 1.3	0.2 ± 2.0	1.1 ± 0.5	3.0 ± 1.6	0.6 ± 0.4	7.6 ± 1.5	0.1 ± 0.0	4.8 ± 3.6	16 ± 7	0.5 ± 0.3
MCOG	0.3 ± 0.2	6.4 ± 1.7	0.7 ± 0.2	0.5 ± 0.2	0.9 ± 0.4	0.1 ± 0.1	4.0 ± 0.9	0.3 ± 0.3	0.9 ± 0.1	4.7 ± 4	0.1 ± 0.1

https://doi.org/10.5194/egusphere-2024-104
Preprint. Discussion started: 17 January 2024

325

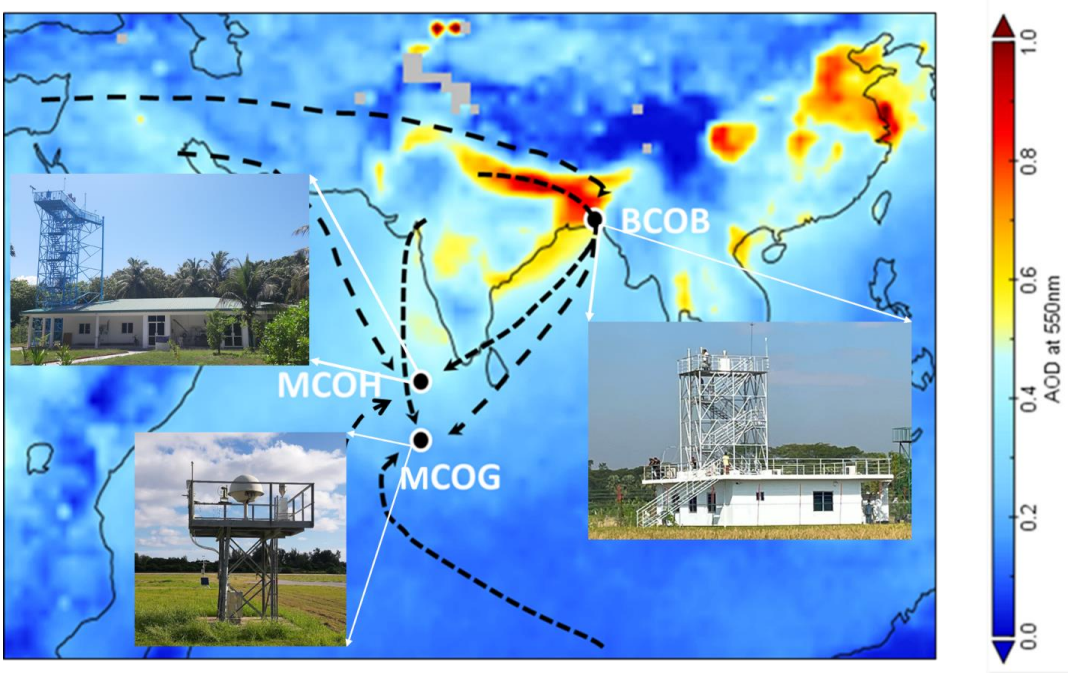

Figure 1. Average Aerosol Optical Depth (AOD) at 550 nm from Moderate Resolution Imaging Spectroradiometer (MODIS) during SAPOEX-18 from December 2017 to March 2018 over the South Asian region. The receptor sites are shown (black fill, with pictures): the Bhola Climate Observatory in Bangladesh (BCOB), the Maldives Climate Observatory at Hanimaadhoo (MCOH), and the Maldives Climate Observatory at Gan (MCOG). The thick black lines with arrow show mean air mass trajectory clusters (more details in Supporting Information Figures S1 and S4).

330

https://doi.org/10.5194/egusphere-2024-104
Preprint. Discussion started: 17 January 2024

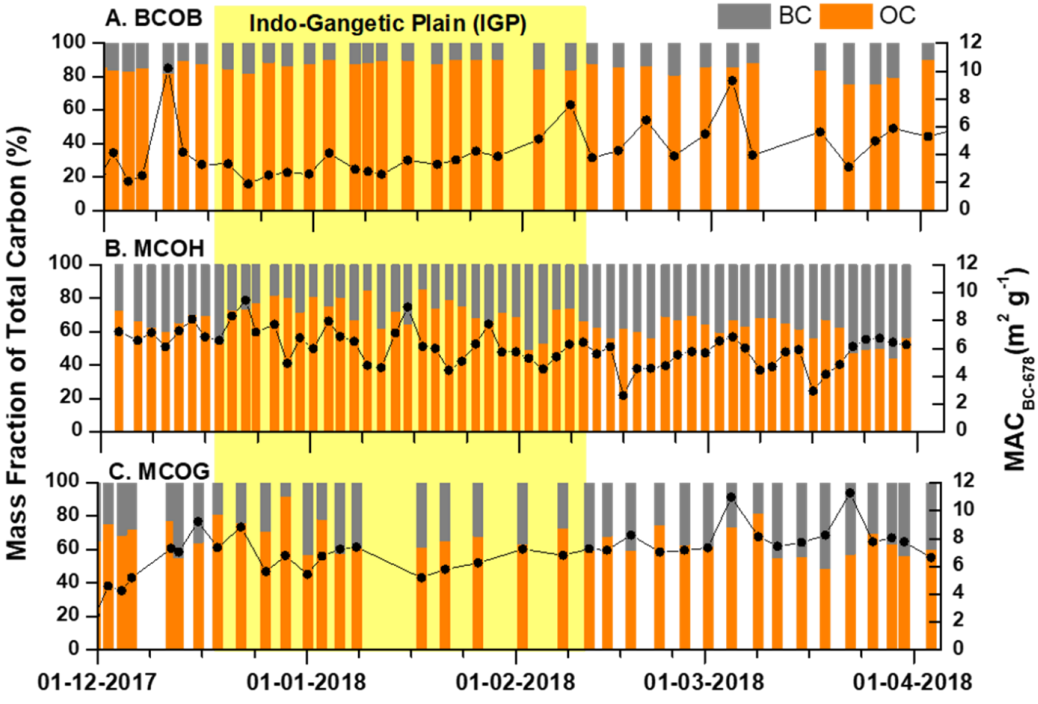

Figure 2. Mass fraction of total carbon (black carbon + organic carbon) and BC mass absorption cross-section (BC-MAC, at 678nm) was measured at three receptor sites in South Asia, i.e., A. Bhola Climate Observatory-Bangladesh (BCOB), B. Maldives Climate Observatory-Hanimaadhoo (MCOH) and C. Maldives Climate Observatory-Gan (MCOG) from 1 December 2017 to early April 2018. The vertical yellow field indicates predominance of air mass origin from the high-pollution source region Indo-Gangetic Plain (IGP).

https://doi.org/10.5194/egusphere-2024-104
Preprint. Discussion started: 17 January 2024

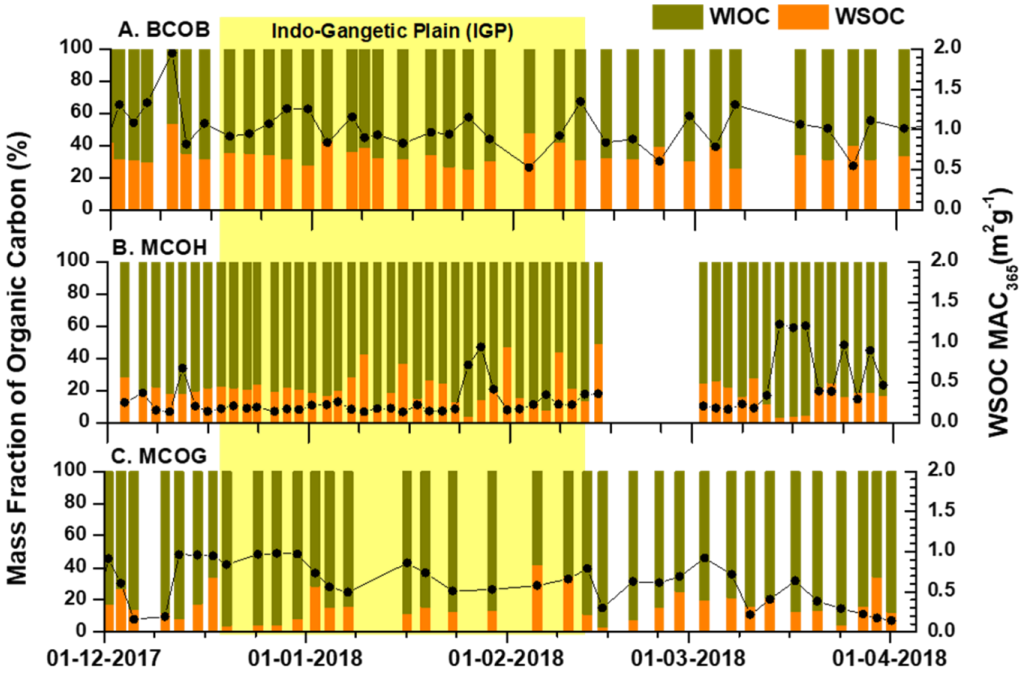

Figure 3. Mass fraction of organic carbon (divided as water-insoluble organic carbon vs water-soluble organic carbon) and mass absorption cross-section for Brown Carbon (Br-C MAC, at 365 nm) measured at three receptor sites in South Asia, i.e., A. Bhola Climate Observatory-Bangladesh (BCOB), B. Maldives Climate Observatory-Hanimaadhoo (MCOH) and C. Maldives Climate Observatory-Gan (MCOG) from 1 December 2017 to early April 2018. The vertical yellow bar indicates predominance of air mass origin from the high-pollution source region Indo-Gangetic Plain (IGP).

https://doi.org/10.5194/egusphere-2024-104
Preprint. Discussion started: 17 January 2024

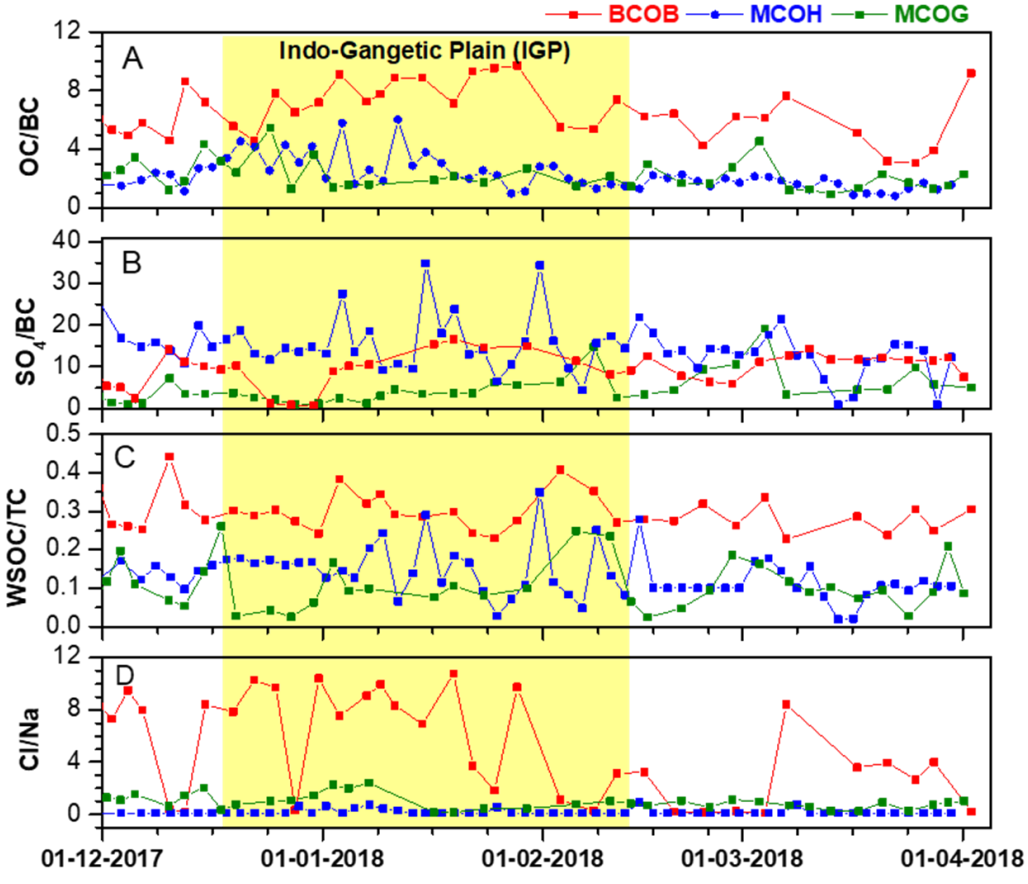

345 **Figure 4. Time series of ratio of measured chemical species OC/EC (panel A), SO_4/BC (panel B), WSOC/BC (panel C), and Cl/Na (panel D, sea water ratio 1.1) over three receptor sites in South Asia, i.e., Bhola Climate Observatory-Bangladesh (BCOB), Maldives Climate Observatory-Hanimaadhoo (MCOH) and Maldives Climate Observatory-Gan (MCOG).**

https://doi.org/10.5194/egusphere-2024-104
Preprint. Discussion started: 17 January 2024

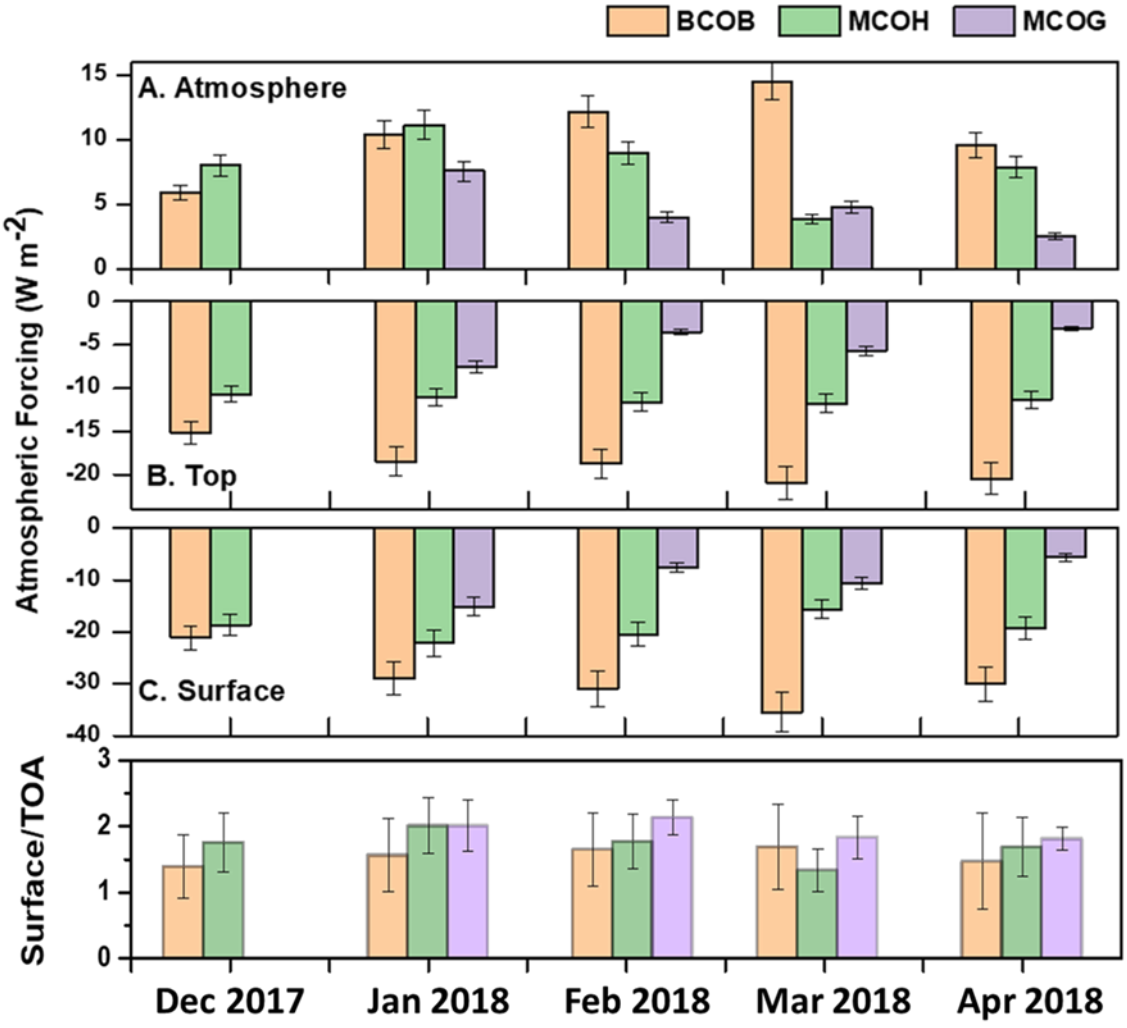

Figure 5. The monthly-average direct aerosol radiative forcing (cloud-free atmosphere) calculated for locations of Bhola Climate Observatory-Bangladesh (BCOB), Maldives Climate Observatory-Hanimaadhoo (MCOH), and Maldives Climate Observatory-Gan (MCOG) from December 2017 to April 2018. A. Atmosphere forcing, B. Top of the atmosphere (TOA) forcing, C. Surface forcing, D. the ratio of surface forcing to top of the atmosphere.

https://doi.org/10.5194/egusphere-2024-104
Preprint. Discussion started: 17 January 2024

References

Ahmed, M., Das, M., Afser, T., Rokonujjaman, M., Akther T., Salam, A.: Emission of Carbonaceous Species from Biomass Burning in the Traditional Rural Cooking Stove in Bangladesh. Open J. Air Pollut., 7, 287–297, https://doi.org/10.4236/ojap.2018.74014, 2018.

Andreae, M. O.: Soot carbon and excess fine potassium: long-range transport of combustion-derived aerosols. Science 220 (4602), 1148–1151, https://doi.org/10.1126/science.220.4602.1148, 1983.

Andreae, M. O. and Gelencser, A.: Black carbon or brown carbon? the nature of light-absorbing carbonaceous aerosols. Atmos. Chem. Phys., 6, 3131–3148, https://doi.org/10.5194/acp-6-3131-2006, 2006.

Ansari, K. and Ramachandran S.: Aerosol characteristics over Indo-Gangetic Plain from ground-based AERONET and MERRA-2/CAMS model simulations. Atmos. Environ., 293, 119434, https://doi.org/10.1016/j.atmosenv.2022.119434, 2023.

Bedareva, T. V., Sviridenkov, M. V., Zhuravleva, T. B.: Retrieval of dust aerosol optical and microphysical properties from ground-based sun-sky radiometer measurements in an approximation of randomly oriental spheroids. J. Quant. Spectrosc. Radiat. Transf. 146, 140–157, http://dx.doi.org/10.1016/j.jqsrt.2014.05.006, 2014.

Bikkina, S. and Sarin, M. M.: $PM_{2.5}$, EC, and OC in the atmospheric outflow from the Indo-Gangetic Plain: Temporal variability and aerosol organic carbon-to-organic mass conversion factor. Sci. Tot. Environ., 487(1), 196–205, https://doi.org/10.1016/j.scitotenv.2014.04.002, 2014.

Bikkina, S, and Sarin, M. M.: Light absorption organic aerosols (brown carbon) over the tropical Indian Ocean: impact of biomass burning emissions. Environ. Res. Lett., 8, 044042, https://doi.org/10.1088/1748-9326/8/4/044042, 2013.

Birch, M. E., Cary, R. A.: Elemental Carbon-Based Method for Monitoring Occupational Exposures to Particulate Diesel Exhaust. Aerosol Sci. Technol., 25, 221–241, https://doi.org/10.1080/02786829608965393,1996,

Bollasina, M. A., Ming, Y., Ramaswamy, V.: Anthropogenic Aerosols and the Weakening of the South Asian Summer Monsoon. Science, 334, 502-505, https://doi.org/10.1126/science.1204994, 2011.

Bosch, C., Andersson, A., Kirillova, E. N., Budhavant, K., Tiwari, S., Praveen, P. S., Russell, L. M., Beres, N. D., Ramanathan, V., Gustafsson, Ö.: Source-diagnostic dual-isotope composition and optical properties of water-soluble organic carbon and elemental carbon in the South Asian outflow intercepted over the Indian Ocean. J. Geophys. Res. Atmos., 119, 11743 –11759, https://doi.org/10.1002/2014JD022127, 2014.

Budhavant, K., Andersson, A., Bosch, C., Krusa, M., Kirillova, E. N., Sheesley, Safai, P.D., Rao, P. S. P., Gustafsson, Ö.: Radiocarbon-based source apportionment of elemental carbon aerosols at two South Asian receptor observatories over a full annual cycle. Environ. Res. Lett., 10, 064004, http://dx.doi.org/10.1088/1748-9326/10/6/064004, 2015.

https://doi.org/10.5194/egusphere-2024-104
Preprint. Discussion started: 17 January 2024

Budhavant, K., Andersson, A., Holmstrand, H., Satheesh, S.K., Gustafsson, Ö. Black carbon aerosols over Indian Ocean have unique source fingerprints and optical characteristics during monsoon season. Proc. Natl. Acad. Sci. 2023, 120 (8) e2210005120, http://doi.org/10.1073/pnas.221000512, 2023.

Budhavant, K., Bikkina, S., Andersson, A., Asmi, E., Kesti, J., Zahid, H., Satheesh, S.K., Gustafsson Ö.: Anthropogenic fine aerosols dominate the wintertime regime over the northern Indian Ocean. Tellus B, 70, 1464871, http://dx.doi.org/10.1080/16000889.2018.14648711, 2018.

Chakrabarty, R. K., Gyawali, M., Yatavelli, R. L. N., Pandey, A., Watts, A. C.: Brown carbon aerosols from burning of boreal peatlands: microphysical properties, emission factors, and implications for direct radiative forcing. Atmos. Chem. Phys., 16, 3033–3040, https://doi.org/10.5194/acp-16-3033-2016, 2008.

Chen, B., Bai, Z., Cui, X., Chen, J., Andersson, A., Gustafsson, G.: Light absorption enhancement of black carbon from urban haze in northern China winter. Environ. Pollut., 221, 418-426, https://doi.org/10.1016/j.envpol.2016.12.004, 2017.

Chen, Y. and Bond, T.C.: Light absorption by organic carbon from wood combustion. Atmos. Chem. Phys., 10, 1773-1787, https://doi.org/10.5194/acp-10-1773-2010, 2010.

Cheng, Y., He, K. B., Zheng, F. K., Duan, Z. Y., Du, Y.L., Ma, J. H., Tan, F. M., Yang, J. M., Liu, X. L., Zhang, R. J., Weber, M. H., Bergin, Russell, A. G. Mass absorption efficiency of elemental carbon and water-soluble organic carbon in Beijing, China. Atmos. Chem. Phys., 11, 11497–11510, https://doi.org/10.5194/acp-11-11497-2011, 2011.

Corbett, J. J. and Koehler, H. W.: Updated emissions from ocean shipping. J. Geophys. Res. Atmos., 108 (D20), https://doi.org/10.1029/2003JD003751, 2003

Corrigan, C. E., Ramanathan V., Schauer. J. J.: Impact of monsoon transition on the physical and optical properties of aerosols. J. Geophys. Res., 111, D18208, https://doi.org/10.1029/2005JD006370, 2006.

Cui, X., Wang, X., Yang, L., Chen, B., Chen, J., Andersson, A., Gustafsson, Ö.: Radiative absorption enhancement from coating on black carbon aerosols. Sci. Tot. Environ. 51-56, 551-552, https://doi.org/10.1016/j.scitotenv.2016.02.026, 2016.

Dasari, S, Andersson, A., Stohl, A., Evangeliou, N., Bikkina, S., Holmstrand, H., Budhavant, K., Salam, A., Gustafsson, Ö.: Source quantification of South Asian black carbon aerosols with isotopes and modelling. Environ. Sci. Technol. 54, 11771–11779, https://doi.org/10.1021/acs.est.0c02193, 2020.

Dasari, S., Andersson, A., Bikkina, S., Holmstrand, H., Budhavant, K., Satheesh, S., Backman, J., Kesti, J., Asmi, E., Salam, A., Bisht, D.S., Tiwari, S., Zahid, A., Gustafsson, Ö.: Photochemical degradation affects the light absorption of water-soluble brown carbon in the South Asian outflow. Sci. Adv. 5, eaau8066, https://doi.org/10.1126/sciadv.aau8066, 2019.

Draxler, R. R.: HYSPLIT 4 user's guide, NOAA Tech. Memo. ERL ARL-230, NOAA Air Resources Laboratory, Silver Spring, 1999.

Draxler, R. R., Hess, G. D.: Description of the HYSPLIT 4 modeling system, NOAA Tech. Memo. ERL ARL-224, NOAA Air Resources Laboratory, Silver Spring, MD, 1997.

Gopikrishnan, G. S. and Kuttippurath, J.: A decade of satellite observations revealed a significant increase in atmospheric formaldehyde from shipping in the Indian Ocean. Atmos. Environ., 246, 118095, https://doi.org/10.1016/j.atmosenv.2020.118095, 2021.

Gustafsson, O., Krusa, M., Zencak, Z., Sheesley, R. J., Granat, L., Engstrom, E., Praveen, P.S., Leck, C., Rodhe, H.: Brown Clouds over South Asia: Biomass or Fossil Fuel Combustion? Science, 2009, 323 (5913), 495–498, https://doi.org/10.1126/science.1164857.

Gustafsson, Ö. and Ramanathan, V.: Convergence on climate warming by black carbon aerosols. Proc. Natl Acad. Sci., USA 113, 4243–4245, https://doi.org/10.1073%2Fpnas.1603570113, 2016.

Hopner, F., Bender, F.A.M., Ekman, A.M.L., Praveen, P.S., Bosch, C., Orgen, A., Andersson, A., Gustafsson, Ö, Ramanathan V.: Vertical profiles of optical and microphysical particle properties above the northern Indian Ocean during CARDEX 2012. Atmos. Chem. Phys., 16, 1045–1064, https://doi.org/10.5194/acp-16-1045-2016, 2016.

Guttikunda, S. K. and Jawahar, P.: Atmospheric emissions and pollution from the coal-fired thermal power plants in India. Atmos. Environ., 92, 449–460, https://doi.org/10.1016/j.atmosenv.2014.04.057, 2014.

Hess, M., Koepke, P., Schult, I. Optical properties of aerosols and clouds: The software package OPAC. Bull. Amer. Meteor. Soc., 79, 831–844, https://doi.org/10.1175/1520-0477(1998)079%3C0831:OPOAAC%3E2.0.CO;2, 1998.

Hoffer, A, Gelencser, A., Guyon, P., Kiss, G., Schmid, O., Frank, G.P., Artaxo, P., Andreae.: Optical properties of humic-like substances (HULIS) in biomass-burning aerosols, Atmos. Chem. Phys., 6, 3563-3570, https://doi.org/10.5194/acp-6-3563-2006, 2006.

Holben, B. N., Eck, T. F., Slutsker, I., Smirnov, A.: AERONET- a federal instrument network and data archive for aerosol characterization. Remote Sens. Environ. 1998, 66, 1–16.

Hopner F., Bender A. M., Ekman, A. M. L., Praveen, P. S., Bosch, C., Orgen, Andersson, A., Kaskaoutis, D. G., Kumar, S., Sharma, D., Singh, R. P., Kharol, S. K.: Effects of crop residue burning on aerosol properties, plume characteristics, and long-range transport over northern India. J. Geophys. Res. Atmos., 119(9), 5424–5444, https://doi.org/10.1002/2013JD021357, 2014.

IPCC, Climate Change 2021: The Physical Science basis. Contribution of Working Group I to the Sixth Assessment Report of the Intergovernmental Panel on Climate Change [Masson-Delmotte, V., P. Zhai, A. Pirani, S. L. Connors, C. Pean, S. Berger, et al., (eds)] Cambridge University Press (2021).

Jacobson, M. C., Hansson, H. C., Noone, K.J., Charlson, R. J.: Organic atmospheric aerosols: review and state of the science. Rev. Geophys., 38, 267-294, https://doi.org/10.1029/1998RG000045, 2000.

Keene, W. C., Pszenny, A. P., Galloway, J. N., Hawley, M. E.: Sea-salt corrections and interpretation of constituent ratios in marine precipitation. J. Geophys. Res. Atmos., 91(D6), 6647. https://doi.org/10.1029/JD091iD06p06647, 1986.

https://doi.org/10.5194/egusphere-2024-104
Preprint. Discussion started: 17 January 2024

Kirillova, E. N., Andersson, A., Tiwari, S., Kumar Srivastava, A., Singh Bisht, D., Gustafsson, Ö.: Water-soluble organic carbon aerosols during a full New Delhi winter: Isotope-base source apportionment and optical properties. J. Geophys. Res. Atmos., 119, 3476–3485, https://doi:10.1002/2013JD020041, 2014.

Kirillova, E. N., Marinoni, A., Bonasoni, P., Vuillermoz, E., Faccchini, M. C., Fuzzi, S., Decesari, S.: Light absorption properties of brown carbon in the high Himalayas.: J. Geophys. Res. Atmos., 121, 9621–9639, https://doi.org/10.1016/j.envpol.2020.114239, 2016

Kirillova, E.N., Andersson, A., Sheesley, R.J., Kruså, M., Praveen, P.S., Budhavant, K., Safai, P.D., Rao, P.S.P., Gustafsson, Ö.: ^{13}C- and ^{14}C-based study of sources and atmospheric processing of water-soluble organic carbon (WSOC) in South Asian aerosols. J. Geophys. Res. Atmos., 118, 614–626, https://doi.org/10.1002/jgrd.50130, 2013.

Knox, A., Evans, G. J., Brook, J. R., Yao, X., Jeong, C. H., Godri, K. J. et al.: Mass Absorption Cross-Section of Ambient Black Carbon Aerosol in Relation to Chemical Age. Aerosol Sci. Technol., 43, 522–532, https://doi.org/10.1080/02786820902777207, 2009.

Kuttippurath, J., Patel, V. K., Pathak, M., Singh, A.: Improvements in SO_2 pollution in India: role of technology and environmental regulations. Environ. Sci. Pollut. Res., 29, 78637–78649, https://doi.org/10.1007/s11356-022-21319-2, 2022.

Lambe, A. T., Cappa, C. D., Massoli, P., Onasch, T. B., Forestieri, S.D., Martin, A. T., Cummings M. J., Croasdale D. R., Brune, W. H., Worsnop, D. R., Davidovits P.: Relationship between oxidation level and optical properties of secondary organic aerosols. Environ. Sci. Technol., 47(12), 6349-6357, https://doi.org/10.1021/es401043j, 2013.

Lelieveld, J., Evans, J. S., Fnais, M., Giannadaki, D., Pozzer, A.: The contribution of outdoor air pollution sources to premature mortality on a global scale. Nature, 367-371, 525 (7569), https://doi:10.1038/nature15371, 2015.

Lu, F., Chen, S., Hu, Z., Han, Z., Alam, K., Luo, H., BI, H., Chen, J., Guo, K.: Sensitivity and uncertainties assessment in radiative forcing due to aerosol optical properties in diverse locations in China. Sci. Tot. Environ., 860, 160447. https://doi.org/10.1016/j.scitotenv.2022.160447, 2023.

Mauderly, J. L. and Chow, J. C.: Health effects of organic aerosols. Inhal Toxicol., 20(3), 257–288. https://doi:10.1080/08958370701866008, 2008.

Nair, H., Budhavant, K., Manoj, M.R., Andersson, A., Satheesh, S.K., Ramanathan, V., Ö. Gustafsson, Ö.: Aerosol demasking enhances climate warming over South Asia. NPJ Clim. Atmos. Sci., 6, 39, https://doi.org/10.1038/s41612-023-00367-6, 2023.

Paris, R., Desboeufs, K.V., Formenti, P., Nava, S., Chou, C.: Chemical characterization of iron in dust and biomass burning aerosols during AMMA-SOP0/DABEX: implication for iron solubility. Atmos. Chem. Phys., 10, 4273–4282, https://doi.org/10.5194/acp-10-4273-2010, 2010.

Pathak, G., Nichter, M., Hardon, A., Moyer, E., Latkar A., Simbaya, J., Pakasi, D., Taqueban, E., Love, J.: Plastic pollution and the open burning of plastic wastes. Glob. Environ. Change, 80, 102648, https://doi.org/10.1016/j.gloenvcha.2023.102648, 2023.

https://doi.org/10.5194/egusphere-2024-104
Preprint. Discussion started: 17 January 2024

Peng, J. F., Hu, M., Guo, S., Du, Z., Zheng, J., Shang, D. Zamora, M. L., Zeng, L., Shao, M., Wu, Y. S., Zheng, J., Wang, Y., Glen, C. R., Collins, D. R., Molina, M. J., Zhang, R. Markedly enhanced absorption and direct radiative forcing of black carbon under polluted urban environments. Proc. Natl. Acad. Sci., 113(16), 4266–4271, https://doi.org/10.1073/pnas.1602310113, 2016.

Ram, K. and Sarin, M.M.: Absorption coefficient and site-specific mass absorption efficiency of elemental carbon in aerosols over Urban, Rural, and high-altitude sites in India. Environ. Sci. Technol., 43(21), 8233–8239, https://doi.org/10.1021/es9011542, 2009.

Ramanathan, V., Chung, C., Kim, D., Bettge, T., Kiehl, J.T., Washington, W.M., Fu, Q., Sikka, D.R., Wild, M.: Atmospheric brown clouds: Impacts on South Asian climate and hydrological cycle. Proc. Nat. Acad. Sci., 102, 5326-5333, https://doi.org/10.1073/pnas.0500656102, 2005.

Ramanathan, V. and Carmichael, G. Global and regional climate changes due to black carbon. Nat. Geosci, 1(4), 221–227, http://dx.doi.org/10.1038/ngeo156, 2008.

Ramanathan, V., Ramana, M. V., Roberts, G., Kim, D., Corrigan, C., Chung, C., Winker, D. Warming trends in Asia amplified by brown cloud solar absorption. Nature, 448, 575-578, https://doi:10.1038/nature06019, 2007.

Rastogi, N., Satish, R., Singh, A., Kumar, V., Thamban, N., Lalchandani, V., Shukla, A., Vats, P., Tripathi, S.N., Ganguly, D. Diurnal variability in the spectral characteristic and sources of water-soluble brown carbon aerosols over Delhi. Sci. Tot. Environ. 794, 148589, https://doi.org/10.1016/j.scitotenv.2021.148589, 2021.

Ricchiazzi, P., Yang, S., Gautier, C., Sowle, D.: SBDART: A research and teaching tool for plane-parallel radiative transfer in the earth's atmosphere. Bull. Am. Meteorol. Soc. 79: 2101–2114, https://doi.org/10.1175/1520-0477(1998)079%3C2101:SARATS%3E2.0.CO;2, 1998.

Ruellan, S., Cachier, H.: Characterization of fresh particulate vehicular exhausts near a Paris high flow road. Atmos. Environ., 35, 453–468, https://doi.org/10.1016/S1352-2310(00)00110-2, 2001.

Satheesh, S. K.: Radiative forcing by aerosols over Bay of Bengal region. Geophys. Res. Lett., 29, 2083, https://doi.org/10.1029/2002GL015334, 2002.

Satheesh, S. K. and Ramanathan, V.: Large difference in tropical aerosol forcing at the top of the atmosphere and Earth's surface. Nature, 405, 60–63, https://doi:10.1038/35011039, 2000.

Shindell, D., Kulenstierna, J. C., Vignati, E., Dingenen, R. V., Amann, M., Klimount, Z., Anenberg, S. C., Mulller, N., Jansessens-Maenhout, G., Raes, F., et al.: Simultaneously Mitigating Near-Term Climate Change and Improving Human Health and Food Security. Science, 335, 183–189, https://doi.org/10.1126/science.1210026, 2012.

Shohel, M., Kistler, M., Rahman, M. A., Kasper-Giebl, A., Reid J. S., Salam A.: Chemical characterization of PM2.5 collected from a rural coastal island of the Bay of Bengal (Bhola, Bangladesh). Environ. Sci. Pollut. Res., 25, 4558–4569, https://doi.org/10.1007/s11356-017-0695-6, 2018.

https://doi.org/10.5194/egusphere-2024-104
Preprint. Discussion started: 17 January 2024

Stamnes, K., Tsay, S. C., Wiscombe, W., Jayaweera, K.: Numerically stable algorithm for discrete ordinate-method radiative transfer in multiple scattering and emitting layered media. Appl. Opt., 27: 2502–2509, https://doi.org/10.1364/AO.27.002502, 1988.

Stone, E. A., Lough, G.C., Schauer, J.J., Praveen, P.S., Corrigan, C.E., Ramanathan V.: Understanding the origin of black carbon in the atmospheric brown cloud over the Indian Ocean. J. Geophys. Res., 122, D22S23, https://doi.org/10.1029/2006JD008118, 2007.

Weingartner, E., Saathoff, H., Schnaiter, M., Streit, N., Bitnar, B., Baltensperger.: Absorption of light by soot particles: Determination of the absorption coefficient using Aethalometers. J. Aerosol. Sci. 2003, 34(10), 1445–1463, https://doi.org/10.1016/S0021-8502(03)00359-8, 2003.

WHO (2016). Country Estimates on Air Pollution Exposure and Health Impact. World Health Organisation. Online at: http://www.who.int/mediacentre/news/releases/2016/air-pollution-estimates/en/.

Yuan, J., Modini, R. L., Zanatta, M., Herber, A. B., Muller, T., Wehner, B., Poalain, L., Tuch, T., Baltensperger, U., Gysel-Beer, M. Variability in the mass absorption cross-section of black carbon (BC) aerosols is driven by BC internal mixing state at the central European background site (Melpitz, Germany) in winter. Atmos. Chem. Phys., 21, 635-655, https://doi.org/10.5194/acp-21-635-2021, 2021.

Zhang, Y., Zhang, Q., Cheng, Y., Su, H., Li, H., Li, M., Zhang, X., Ding, A., He. K.: Amplication of light absorption of black carbon associated with air pollution. Atmos. Chem. Phys., 18, 9879–9896, https://doi.org/10.5194/acp-18-9879-2018, 2018.